DOI: 10.1002/ejoc.201100720

Effect of Surfactant Structure on Carbon Nanotube Sidewall Adsorption

Antonello Di Crescenzo,[a] Raimondo Germani,[b] Elisa Del Canto,[c] Silvia Giordani,[c] Gianfranco Savelli,[b] and Antonella Fontana*[a]

Dedicated to Professor Gianfranco Scorrano on the occasion of his 72nd birthday

Keywords: Nanotechnology / Nanotubes / Semiconductors / Surfactants / Raman spectroscopy

One conventional and two related gemini surfactants have been used for the preparation of stable single-walled carbon nanotube (SWNT) aqueous dispersions. The surfactants investigated are able to disperse SWNTs at surfactant/carbon nanotube weight ratios far lower than widely used conventional surfactants. The gemini surfactants investigated demonstrated the ability to solubilize a larger amount of SWNTs with respect to the related single-tailed surfactant at concentrations far lower than their critical micellar concentrations. Their selectivity towards semiconducting SWNTs with large diameters was inferred from radial breathing mode Raman data.

Introduction

In the last decade, carbon nanotubes (CNTs) have been the undisputed protagonists of research in the field of nanotechnology. These nanoscale tubular structures, defined as the third allotropic crystalline form of carbon, have made a significant impact on science and technology. Their unique mechanical, optical and electronic properties have applications in materials science[1] as well as in the biomedical field.[2,3] For example, CNTs are deemed as ideal materials for reinforcing fibres due to their exceptional mechanical properties.[4] Moreover, CNT/polymer composites and CNT/ionic liquid gels have been considered for the preparation of actuator systems[5] and reaction media.[6] CNTs have been extensively explored for the development of highly sensitive and specific nanoscale biosensors.[2] Due to their intrinsic stability, structural flexibility and high aspect ratio, CNTs may act as highly efficient vehicles for the transport of a wide range of molecules across living cell membranes.[7] Many studies have shown their suitability as drug carriers[8] in the treatment of various diseases, in particular, cancer.[9] Unfortunately, substantial van der Waals attractions between the tubes lead to their aggregation in large and difficult to process bundles, where the properties of individually dispersed nanotubes are often lost.

In order to improve the dispersibility of CNTs both covalent and noncovalent functionalization approaches have been widely used. The latter is preferred when inherent mechanical, electrical or optical properties of CNTs are to be exploited. Conventional surfactants have been widely used to stabilize CNT dispersions, and particular attention has been devoted to selecting the best dispersing agent in terms of (1) percentage of dispersed CNTs, (2) ratio of dispersing agents vs. dispersed CNTs, (3) stability of the solutions obtained, (4) compatibility with the features of the final material and (5) cost, to mention but a few.

Conventional surfactants are molecules consisting of a hydrophilic head group and a hydrophobic tail.[10] This amphiphilic nature endows surfactants with unique solubilization and interfacial features. Among these properties, most noteworthy is their behaviour in dilute aqueous solutions, where surfactants self-assemble in aggregates with hydrophobic tails segregated from water. The simplest aggregate structure is the spherical micelle.

Micellization occurs above a critical micellar concentration (CMC) and is driven by hydrophobic forces, opposed by electrostatic repulsion between the polar head groups at the micellar surface.[11] These assemblies, with interiors consisting of mobile, nonlinear hydrocarbon chains, provide a nanoheterogeneous two-phase system, characterized by macroscopic homogeneity, widely used for favouring the aqueous solubilization of scarcely soluble substrates. Factors such as the hydrophilic/lipophilic balance of the substrate, the micellar characteristics of the core and surface

[a] Dipartimento di Scienze del Farmaco, Università "G. d'Annunzio",
Via dei Vestini, 66100 Chieti, Italy
Fax: +39-0871-3554790
E-mail: fontana@unich.it
[b] CEMIN, Centro di Eccellenza Materiali Innovativi Nanostrutturati; Dipartimento di Chimica, Università di Perugia,
Via Elce di Sotto, 8, 06123 Perugia, Italy
[c] School of Chemistry/Centre for Research on Adaptive Nanostructures and Nanodevices (CRANN), Trinity College Dublin,
Dublin 2, Ireland

Supporting information for this article is available on the WWW under http://dx.doi.org/10.1002/ejoc.201100720.

and the surface/volume ratio determine the proportion of substrate solubilized in each region.[12]

In the presence of CNTs, self-assembly of surfactants is driven by the affinity of the latter for the CNT sidewalls. In particular, three models of surfactant adsorption have been suggested and considered as reliable: (1) surfactant hemimicelles that sheath the CNT surface,[13] (2) formation of cylindrical surfactant micelles with the nanotube in the centre,[14] whose formation does not proceed by incorporation of a nanotube into the micelle, but by adsorption of vertically oriented molecules onto the nanotube surface, and (3) randomly adsorbed surfactant structures surrounding the nanotubes.[15] Although these models have very different features, all entail a minimization of the interfacial energy of the nanotube–water interface.[16] This minimization is prevailingly reached by van der Waals and CH–π interactions between the hydrophobic tails of the surfactant and the sidewalls of CNTs. Meanwhile, hydrophilic head groups provide water solubility by pointing towards the aqueous phase.

In this work, a conventional single-tailed surfactant, *N*-[*p*-(*n*-dodecyloxybenzyl)]-*N*,*N*,*N*-trimethylammonium bromide (pDOTABr), and two related gemini surfactants, 2,5-bis(*n*-dodecyloxy)-1,4-bis(*N*,*N*,*N*-trimethylammoniomethyl)phenyl bromide [pXDo(TA)$_2$Br] and 2,5-dimethoxy-1,4-bis[*N*-(*n*-dodecyl)-*N*,*N*-dimethylammoniomethyl]phenyl bromide [pXMo(DDA)$_2$Br], have been used as dispersing agents for SWNTs in aqueous solution (Scheme 1). The effect of the surfactant structure on the stability of the dispersion obtained and the adsorption capacity onto the SWNT sidewalls have been investigated.

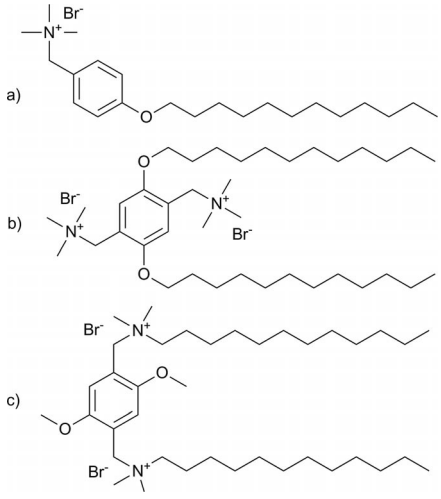

Scheme 1. Structures of a) pDOTABr, b) pXDo(TA)$_2$Br and c) pXMo(DDA)$_2$Br.

Gemini surfactants typically possess two hydrophobic tails and two polar head groups linked by a spacer, which may be rigid or flexible.[11] These surfactants have a great potential thanks to the enormous variability that characterizes their structures[17] and a number of unique aggregation properties in comparison to conventional surfactants, such as (1) lower CMCs, (2) strong dependence on spacer structure and length, (3) strong hydrophobic microdomain and (4) prevailingly micellar aggregate morphology spanning from spherical to disk-like or rod micelles due to their high surfactant packing parameter.[11,17,18] In particular, the aggregate shape strongly depends on the spacer length, i.e. the tendency to form worms rather than spherical micelles increases with the shortening of the spacer and chain lengths.[11] For this reason gemini surfactants are expected to exhibit quite different interactions with CNTs with respect to conventional surfactants. To the best of our knowledge, few papers have been devoted to the study of interaction of gemini surfactants with CNTs.[18,19] In addition, all of these have considered only gemini surfactants with a flexible alkyl spacer. We present gemini surfactants characterized by an aromatic spacer. Aromatic moieties have been demonstrated to strongly interact with CNTs.[13] The benzene ring has been proposed to be one of the main reasons for the high dispersive efficiency of sodium dodecylbenzene sulfonate (sdbs) with respect to sodium dodecyl sulfate (sds).[13] Analogously, pyrene derivatives have been shown to favour the solubilization of SWNTs[16c,20] and allow supramolecular attachment onto the nanotube surface of a variety of molecules.[21] Indeed π–π stacking interactions between the aromatic core of the adsorbing dispersant and the nanotube surface have been demonstrated[16c,22] to be conclusive for the adsorption and, in this case, could, in principle, significantly alter the previously described simple hydrophobic gemini surfactant/CNT interactions. Our data demonstrate that the surfactants investigated are very good dispersing agents being able to disperse CNTs at exceptionally low surfactant/CNT weight ratios [1.5, 1.7 and 2.4 for pDOTABr, pXDo(TA)$_2$Br and pXMo(DDA)$_2$Br, respectively]. It is worth noting that conventional surfactants, such as cetyltrimethylammonium bromide (ctaBr), sds and sdbs, disperse CNTs at surfactant/CNT weight ratios at values around or higher than ten.[23,24]

Results and Discussion

Characterization of the Surfactants Investigated

The gemini surfactants investigated are less soluble in water with respect to the single-tailed cationic analogues. Solubilities of 0.05 and 0.06 M have been determined[25] for pXDo(TA)$_2$Br and pXMo(DDA)$_2$Br at room temperature, respectively, whereas pDOTABr is completely soluble in water. Literature CMC values, determined by conductivity or tensiometry methods, are 0.44,[25] 0.66[25] and 0.55[26] mM for pXDo(TA)$_2$Br, pXMo(DDA)$_2$Br and pDOTABr, respectively. Degrees of ionization, α, much higher than those of the corresponding monocationic bromides have been determined[25] for micellar solutions of the surfactants [0.32, 0.40 and 0.25[27] for pXDo(TA)$_2$Br, pXMo(DDA)$_2$Br and pDOTABr, respectively].

Dispersing Ability of the Surfactants Towards SWNTs

Aqueous dispersions of SWNTs were prepared by adding 5 mL of aqueous dispersant solutions of different concen-

trations to 1 mg of pristine SWNTs. The samples were then sonicated for 5 h and the suspensions were centrifuged at 4000 rpm for 15 min to remove large bundles of SWNTs and/or residual metal catalysts from the supernatant aqueous solution containing exfoliated SWNTs or small bundles. All three surfactants were quite good SWNT dispersants at room temperature as shown in Figure 1, which was confirmed by the well-resolved van Hove transitions evident in UV/Vis/NIR absorption spectra normalized at 800 nm (Figure 2).

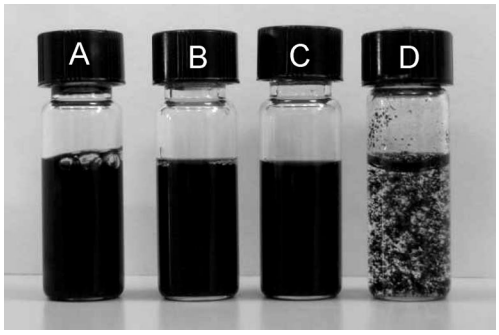

Figure 1. Aqueous dispersions of SWNTs (0.2 mg/mL) obtained by sonication (5 h) with 1 mM aqueous solutions of (A) pDOTABr, (B) pXDo(TA)$_2$Br, (C) pXMo(DDA)$_2$Br and (D) in the absence of surfactant.

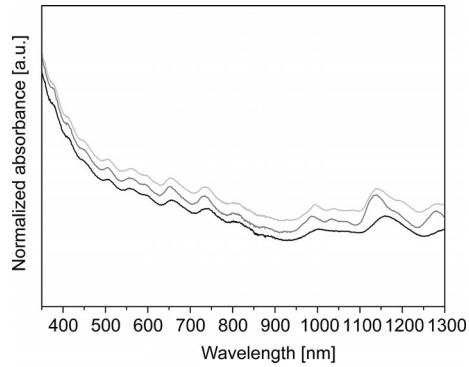

Figure 2. UV/Vis/NIR absorbance spectra of aqueous SWNT dispersions prepared with 0.5 mM pDOTABr (black), 0.75 mM pXDo(TA)$_2$Br (dark grey) and 0.75 mM pXMo(DDA)$_2$Br (light grey). Spectra are shifted vertically by 0.04 a.u. in order to highlight comparisons and differences. The initial amount of SWNTs was 1 mg in each sample.

UV/Vis spectroscopy has also been used to quantify the amount of exfoliated SWNTs dispersed in the aqueous surfactant solution by exploiting the previously determined[23] extinction coefficient of $(106.0 \pm 1.3)\ mL\,mg^{-1}\,cm^{-1}$ at 377 nm, a wavelength where none of the surfactants investigated absorb. Figure 3 reports the percentage of dispersed SWNTs against the concentration of the dispersants. Although the single-chain surfactant appears not to be able to effectively disperse SWNTs below its CMC, the gemini surfactants disperse nanotubes even at surfactant concentrations well below their CMC values. A similar result has been already highlighted in a previous study[18] where gemini surfactant hexyl-α,ω-bis(dodecyldimethylammonium) bromide disperses CNTs at concentrations well below its CMC compared to its single-tailed analogue. The authors attributed this CNT dispersing ability to the higher charge capacity, stronger adsorption ability and compact alignment on the nanotube surface of the gemini than the single-tailed surfactant. Indeed, in the conventional surfactant, the single ammonium ion is exposed to the aqueous solution, favouring the dispersion of the nanotube in the aqueous medium, whereas the benzene ring and alkyl chain in-

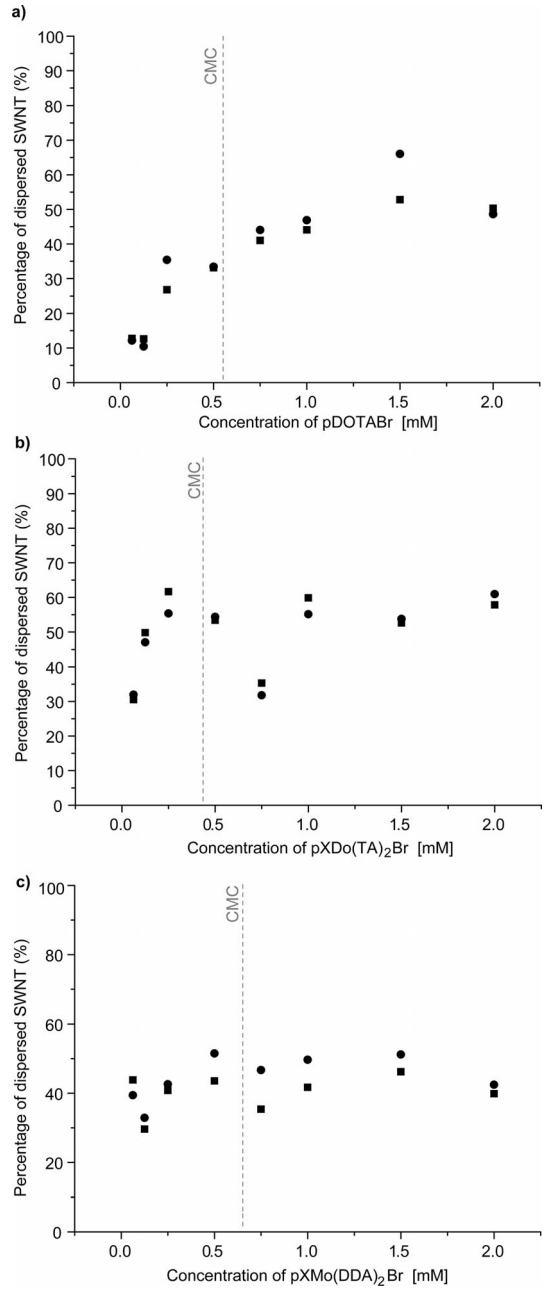

Figure 3. Percentage of SWNTs dispersed with a) pDOTABr, b) pXDo(TA)$_2$Br and c) pXMo(DDA)$_2$Br (real absorbance/theoretical absorbance determined at 377 nm taking advantage of the calibration curve constructed by Di Crescenzo et al.[23] with $\varepsilon_{377\ nm}$ = 106.0 mL/mg cm). Circles and squares refer to different experiments performed under the same experimental conditions.

teract with the nanotube backbone by π–π stacking and van der Waals interactions, respectively. The appearance of enhanced suspension of SWNTs only above the CMC of pDOTABr could be ascribed either to the formation of charged hemimicelles along the SWNTs or to tail-to-tail hydrophobic interactions between the surfactant alkyl chains with the formation of a dense adsorbed monolayer around the SWNTs. In both cases the role of surfactant aggregation for the effect to be manifest appears to be crucial. Nevertheless the former arrangement is quite unlikely because of the inherent difficulty of packing such relatively large molecules on nanotubes of relatively small diameters.[14] In the case of gemini surfactants, the dispersion is ensured, at a concentration well below the CMC, by stronger hydrophobic interactions between the two alkyl chains and the CNT backbone and the higher charge capacity per single molecule of surfactant. Indeed, gemini surfactants have α values much higher than the corresponding monocationic bromides and are known[11] to exhibit favourable packing, due to the capacity of the spacer to force the pair of ionic groups to reside in a less space-filling geometry relative to that of two conventional surfactants.

pXDo(TA)$_2$Br appears to be the best dispersant investigated, capable of solubilizing twice as much SWNTs as pDOTABr and almost one and a half times as much as pXMo(DDA)$_2$Br at a concentration of 0.25 mM. In fact, pXDo(TA)$_2$Br ensures excellent exfoliation through repulsive electrostatic interactions by the two flanking charged ammonium ions. Vice versa, the decreased dispersing ability observed for pXDo(TA)$_2$Br at 0.75 mM may be due to the preference of this surfactant, at a concentration just above the CMC, to form micelles rather than adsorb on to the nanotube surface. By inspecting the data reported in Figure 3 (b), a maximum dispersion of SWNTs is exhibited by pXDo(TA)$_2$Br at 0.25 mM. The concentration of 0.25 mM is therefore the maximum concentration of adsorbed pXDo(TA)$_2$Br. It is noteworthy that 0.75 mM corresponds exactly to a concentration of free surfactant in solution equal to its CMC once the amount of adsorbed surfactant has been disregarded. Actually, it has been previously demonstrated that the dispersibility of SWNTs in water depends both on the affinity of the surfactant for the nanotube surface and its solubility in water and that micelles could be the main cause of nanotube aggregation at sds concentration above its CMC.[16c,28]

In order to assess the different behaviour and the subsequent different adsorbing capacity of the surfactants investigated towards the SWNT sidewalls, we monitored the resulting dispersions by emission spectroscopy. The three surfactants are fluorescent and show a characteristic emission spectrum in the 200–500 nm range [λ_{exc} = 277, 316 and 313 nm for pDOTABr, pXDo(TA)$_2$Br and pXMo(DDA)$_2$Br, respectively]. A substantial decrease of fluorescence emission of these dispersants can be monitored when SWNTs are present in the dispersion (see Figure 4). This decrease is probably due to the static quenching of the molecules whose chromophore group interacts by π–π stacking interactions with the carbon nanotube backbone.

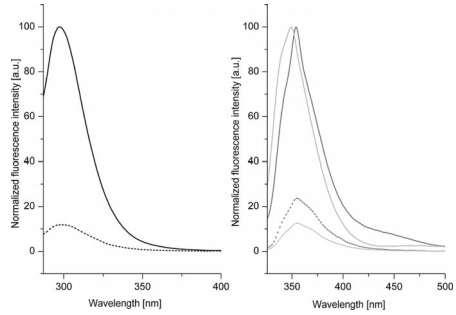

Figure 4. Fluorescence intensity of 0.1 mM aqueous surfactant pDOTABr (black), pXDo(TA)$_2$Br (dark grey) and pXMo(DDA)$_2$Br (light grey), in the absence (solid line) and in the presence (dashed line) of SWNTs (5 μg/mL).

The good dispersing ability of the surfactants was additionally confirmed by NIR–photoluminescence (PL) spectroscopy. Structured emission features can be seen in the spectra of the three dispersions (Figure 5 and Figure S1 in the Supporting Information). Following the experimental Kataura plot[29] assignment of individual optical frequencies bands to specific nanotubes, the NIR–PL spectra do not highlight any notable selectivity within semiconduct-

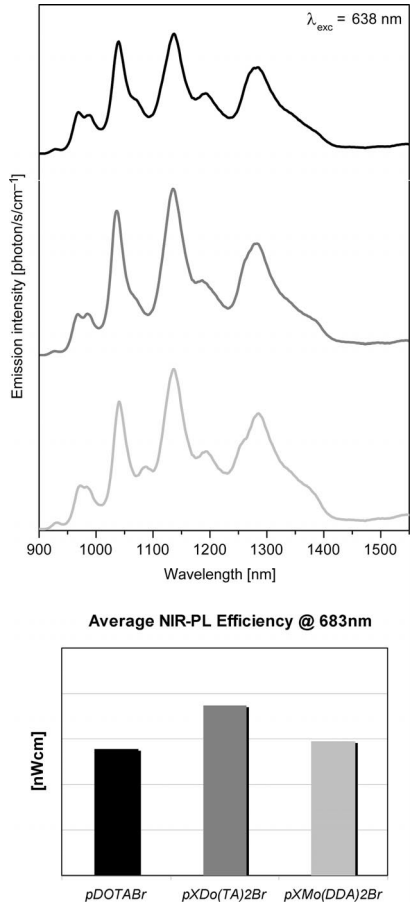

Figure 5. NIR–PL spectra (λ_{exc} = 638 nm) of SWNTs solubilised with pDOTABr (black), pXDo(TA)$_2$Br (dark grey) and pXMo(DDA)$_2$Br (light grey). The histogram reports the NIR–PL efficiency of SWNTs dispersed with the investigated dispersants.

ing SWNTs of different diameters. NIR–PL efficiency data shown in Figure 5 suggest pXDo(TA)$_2$Br as the best dispersant of the three surfactants investigated.

Raman spectra have also been recorded (Figure S2). The I_D/I_G ratios of the dispersed SWNTs are very similar to that of the raw material, suggesting that sonication did not strongly affect the nanotube integrity. The radial breathing mode bands (RBM) of the recorded Raman spectra upon excitation at 488 nm are reported in Figure 6. Experimental Kataura plots[30] allow the assignment of the individual RBM bands at 203 cm^{-1} to (9,8) and (13,3) large semiconducting tubes. The intensity decrease appears to be associated with some type of metallic nanotubes. The spectra highlight decreased relative intensities of the bands associated with small diameter metallic tubes resonant in the RBM region > 220 cm^{-1} with respect to raw and sdbs-coated SWNTs. Upon excitation at 633 nm (Figure S3), the Raman spectra confirm the decreased relative intensities of the bands associated with metallic tubes. In the latter case the decrease of relative intensities involves CNTs of larger diameters resonant in the RBM region < 220 cm^{-1}. The same spectra highlight a small decrease of relative intensities of the bands associated with smaller diameter semiconducting CNTs. These data suggest that the surfactants investigated, and overall gemini surfactants, bring prevailingly large diameter semiconducting SWNTs into solution.

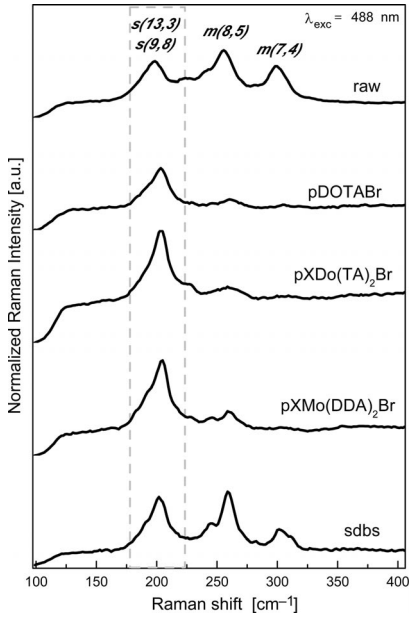

Figure 6. RBM bands in the Raman spectra for raw SWNTs and for SWNTs dispersed in 1 mM pDOTABr, pXDo(TA)$_2$Br, pXMo(DDA)$_2$Br and sdbs. Assignments are based on experimental Kataura plots. All the spectra are normalized on the G band.

In order to confirm whether the intensity change of the RBM band derives from the variation of the concentration of the corresponding CNTs or from the variation of the resonance condition of the recorded spectrum (i.e. the change of the electronic structure of the nanotubes due to the interaction with the dispersants), we performed a comparison of the spectra of the coated nanotubes (after subtraction of the luminescence background) and the spectra of the nanotubes thoroughly washed with acetone. The comparison is depicted in Figure S4, and almost no difference can be detected between the two series of spectra. Therefore, we can draw the conclusion that adsorption with the surfactants investigated leads to some selection of nanotubes, although specific interactions with the dispersing molecules are unlikely. Indeed, there is no difference in selectivity between conventional and gemini surfactants highlighting that, contrary to our expectations, the rigidity and length of the spacer do not play a crucial role.

Stability of the SWNT Aqueous Dispersions

To assess the stability of the SWNT dispersions at room temperature, UV/Vis spectra were monitored over time (Figures S5–S7) and recorded after 10 min centrifugation at 4000 rpm. Over two to three months, the SWNT aqueous dispersions were fairly stable as the SWNT concentration (measured from the absorbance at 377 nm) remained constant in the presence of different surfactant concentrations. A precipitation of ca. 50% of the initially dispersed SWNTs was detected in the sample obtained with pDOTABr well below its CMC (Figure S5).

The ζ-potential is often used as an index of the magnitude of electrostatic interactions between colloidal particles and it is thus considered a further measure of the colloidal stability of a suspension. Colloidal solutions with a ζ-potential of less than –15 mV or more than 15 mV are particularly stable because of electrostatic repulsion interactions.[31] The ζ-potential values for the SWNT solutions prepared with pDOTABr, pXDo(TA)$_2$Br and pXMo(DDA)$_2$Br were 55±4 mV, 60 ± 2 mV and 52 ± 1 mV, respectively. These highly positive values further confirm their stability observed over time.

Conclusions

In conclusion, we have demonstrated a simple protocol to obtain exfoliated and stable suspensions of SWNTs in water in the presence of very low concentrations of gemini surfactants. Indeed, the surfactants investigated are able to disperse SWNTs at surfactant/CNTs weight ratios from four to seven times lower than conventional surfactants such as ctaBr, sds or sdbs. SWNT concentration was increased twofold with respect to the analogous single-tailed surfactant at the lowest effective dispersing concentration of the surfactant. Gemini surfactants show a slightly pronounced selectivity towards semiconducting SWNTs, thus paving the way for applications in CNT enrichment or fractionation.

Experimental Section

Materials: Pristine HiPCO SWNTs (lot #0556) were provided by Carbon Nanotechnologies, Inc. Houston, USA and were used as received. All organic reagents and solvents were purchased from

Sigma–Aldrich and were used without further purification. Ultra pure MilliQ water (Millipore Corp. model Direct-Q 3) with a resistivity of >18.2 MΩcm was used to prepare all solutions.

Melting points were determined with a Barloworld Scientific Stewart SMP3 apparatus. GC analyses were performed with an Agilent 6850 Series II Network GC instrument (column DB-35MS l 30 m, d 0.32 mm, film 0.25 μm). TLC was performed on silica gel on aluminium foil. ^{1}H NMR and ^{13}C NMR were recorded with a Bruker AVANCE DRX 400 instrument using $CDCl_3$ or CD_3OD as solvents at 25.0 °C. Chemical shifts are given in ppm relative to the residual solvent signal.

***p*-(Dodecyloxy)benzaldehyde:** To a 1 L round-bottomed flask, equipped with a condenser with a nitrogen inlet, dropping funnel and mechanical stirrer, were introduced 4-hydroxybenzaldehyde (40.0 g, 0.327 mol), anhydrous K_2CO_3 (45.27 g, 0.327 mol) and CH_3CN (400 mL). The mixture was heated to reflux with stirring, and dodecylbromide (71.5 mL, 0.297 mol) was added. The mixture was heated to reflux overnight and, after it was cooled to room temperature, it was treated with H_2O, NaOH and extracted into petroleum ether. The organic phase was dried with Na_2SO_4, decolorized with carbon and filtered. After solvent elimination, the pale yellow oil was crystallized from methanol at –20 °C. The white solid was collected by filtration, washed with cool petroleum ether and finally dried under vacuum at room temperature; yield 90%. M.p. =< 35 °C. GC = 98.8%. ^{1}H NMR (400 MHz, $CDCl_3$): δ = 0.88 (tr, ^3J = 6.8 Hz, 3 H, CH_3), 1.27 (m, 16 H, $8CH_2$), 1.45 (m, 2 H, CH_2), 1.82 (m, 2 H, $2CH_2$), 4.04 (tr, ^3J = 6.8 Hz, 2 H, CH_2O), 7.00 (dd, J = 6.7, 2.0 Hz, 2 H, Ar), 7.84 (dd, J = 6.7, 2.0 Hz, 2 H, Ar), 9.88 (s, 1 H, COH) ppm. ^{13}C NMR (400 MHz, $CDCl_3$): δ = 14.52 (CH_3 chain), 23.09, 26.35, 29.45, 29.74, 29.94, 29.98, 30.04, 32.32 (CH_2 chain), 68.84 (CH_2OAr), 115.15 (*o*-*Ar*OCH_2), 130.14 (*A*rCOH-*ipso*), 132.39 (*o*-*Ar*COH), 164.69 (OAr-*ipso*), 191.23 (Ar-*C*OH) ppm.

***p*-(Dodecyloxy)benzylalcohol:** To a 1 L round-bottomed flask were introduced *p*-(dodecyloxy)benzaldehyde (43.1 g, 0.148 mol), methanol (20 mL) and THF (300 mL) with magnetic stirring. $NaBH_4$ (5.6 g, 0.148 mol) was gradually added, keeping the temperature of the reaction mixture at 40 °C. The mixture was left to stir until gas emission had finished. The reaction was followed by TLC with diethyl ether/petroleum ether, 8:2 (v/v), until a unitary stain was reached. The mixture was treated with H_2O and H_2SO_4 (10%) in order to destroy excess $NaBH_4$, and the product was extracted into diethyl ether. The organic phase was dried with Na_2SO_4, filtered, concentrated by half and cooled to –20 °C. The white crystalline solid was washed with cool petroleum ether and dried under vacuum at room temperature; yield 95%, m.p. 68–70 °C, GC 99%. ^{1}H NMR (400 MHz, $CDCl_3$): δ = 0.89 (tr, ^3J = 6.8 Hz, 3 H, CH_3), 1.28 (m, 16 H, $8CH_2$), 1.46 (m, 2 H, CH_2), 1.80 (m, 2 H, CH_2), 3.96 (tr, ^3J = 6.6 Hz, 2 H, CH_2), 4.63 (s, 2 H, OCH_2), 6.90 (dd, J = 6.68, 2.09 Hz, 2 H, Ar in ortho OR), 7.20–7.30 (dd, J = 6.7, 2.0 Hz, 2 H, Ar) ppm. ^{13}C NMR (400 MHz, $CDCl_3$): δ = 14.52 (CH_3 chain), 23.09, 26.44, 29.67, 29.75, 29.81, 30.00, 30.04, 32.32 (CH_2 chain), 65.54 (ArCH_2O), 68.49 (CH_2OAr), 114.98 (*o*-*Ar*-OCH_2), 129.04 (*o*-*Ar*CH_2OH), 133.29 (*Ar*CH_2OH-*ipso*), 159.23 (OAr-*ipso*) ppm.

***p*-(Dodecyloxy)benzyl Bromide:** To a 1 L round-bottomed flask, equipped with dropping funnel and a magnetic stirrer bar, were introduced *p*-(dodecyloxy)benzyl alcohol (40.7 g, 0.139 mol) and diethyl ether (300 mL). PBr_3 (13.1 mL, 0.139 mol) was introduced with stirring, and the mixture was cooled using an ice/water bath. The reaction was followed by TLC with diethyl ether/petroleum ether, 2:8 (v/v), until a unitary stain was reached. The mixture was treated with water and ice in order to destroy excess PBr_3. The organic phase was washed with water to neutrality, dried with Na_2SO_4, filtered and concentrated. The product, which solidifies when cooled to 0 °C, was used directly in the following step. TLC in petroleum ether gave a single spot, m.p. 49–50 °C.

***N*-[*p*-(*n*-Dodecyloxybenzyl)]-*N*,*N*,*N*-trimethylammonium Bromide (pDOTABr):** To a 1 L glass-stoppered round-bottomed flask were introduced *p*-(dodecyloxy)benzyl bromide (20.0 g, 0.056 mol) and trimethylamine ethanol solution (11% w/v, 69.0 mL, 0.10 mol). The initially heterogeneous mixture was stirred overnight. When TLC confirmed the complete disappearance of the starting materials, the solution was concentrated until a thick oil was obtained. The oil was washed several times with diethyl ether to become a semisolid and recrystallized from dried THF. The solid was collected by filtration, washed with diethyl ether and dried under vacuum at room temperature; yield 93%, m.p. 187–189 °C. CMC = 5.91×10^{-4} M (surface tension; because no minima were observed in the surface tension vs. log[pDOTABr] plot, the surfactant is considered pure), 5.54×10^{-4} M (conductivity). ^{1}H NMR (400 MHz, CD_3OD): δ = 0.90 (tr, ^3J = 6.8 Hz, 3 H, RCH_3), 1.35 (m, 16 H, $8CH_2$), 1.48 (m, 2 H, CH_2), 1.81 (m, 2 H, CH_2), 3.09 [s, 9 H, $N^+(CH_3)_3$], 4.05 (tr, ^3J = 6.4 Hz, 2 H, RCH_2O), 4.49 (s, 2 H, $ArCH_2N$), 7.09 (dd, J = 6.9, 2.0 Hz, 2 H, Ar), 7.48 (d, J = 7 Hz, 2 H, *o*-ArCH_2N^+) ppm. ^{13}C NMR (400 MHz, $CDCl_3$): δ = 13.44 (CH_3 chain), 22.73, 26.13, 29.27, 29.47, 29.70, 29.75, 32.06 (CH_2 chain), 51.80 [$N^+(CH_3)_3$], 68.25 (ArCH_2O), 69.28 (N^+CH_2OAr), 115.11 (*o*-*Ar*OCH_2), 119.64 (*Ar*CH_2N^+-*ipso*), 134.42 (*o*-*Ar*CH_2N^+), 161.59 (OAr-*ipso*) ppm.

The purity of the cationic surfactant with Br^- as the counterion was confirmed also by potentiometric titration with 0.1 M $AgNO_3$ after precipitation of the surfactant with $NaClO_4$ and acidification to pH = 1 with HNO_3 (Br calcd. 19.28%; found 19.20%).

2,5-Bis(*n*-dodecyloxy)-1,4-bis(*N*,*N*,*N*-trimethylammoniomethyl)-phenyl Bromide [pXDo(TA)$_2$Br] and 2,5-Dimethoxy-1,4-bis[*N*-(*n*-dodecyl-*N*,*N*-dimethylammoniomethyl)phenyl Bromide (pXMo-(DDA)$_2$Br): Gemini surfactants were synthesized as reported by Brinchi et al.[25] The compounds have m.p. and ^{1}H NMR spectroscopic data in accordance with those reported.[25]

pXDo(TA)$_2$Br: ^{1}H NMR (400 MHz, CD_3OD): δ = 0.91 (t, ^3J = 6.8 Hz, 6 H, $2CH_3$), 1.30 (m, 32 H, 16 CH_2), 1.50 (m, 4 H, 2 CH_2), 1.87 (m 4 H, 2 CH_2), 3.21 [s, 18 H, 2 $N^+(CH_3)_3$], 4.13 (t, ^3J = 6.8 Hz, 4 H, 2 OCH_2), 4.61 (s, 4 H, 2 CH_2Ar), 7.38 (s, 2 H, Ar) ppm. ^{13}C NMR (400 MHz, CD_3OD): δ = 13.43 (CH_3 chain), 22.73, 26.26, 29.32, 29.47, 29.56, 29.76, 32.06 (CH_2 chain), 52.97 [$N^+(CH_3)_3$], 63.91 (ArCH_2N^+), 69.69 (CH_2OAr), 118.23 (Ar), 120.11 (*ipso*-*Ar*CH_2N^+), 152.50 (OAr-*ipso*) ppm. Br calcd. 21.28%; found 21.30%.

pXMo(DDA)$_2$Br: ^{1}H NMR (400 MHz, CD_3OD): δ = 0.91 (t, ^3J = 6.8 Hz, 6 H, $2CH_3$), 1.31 (m, 32 H, 16 CH_2), 1.41 (m, 4 H, 2 CH_2), 1.92 (m 4 H, 2 CH_2), 3.10 [s, 12 H, 2 $N^+(CH_3)_2$], 3.42 (m, 4 H, 2 N^+CH_2), 3.96 (s, 6 H, 2 OCH_3), 4.60 (s, 4 H, 2 $ArCH_2N^+$), 7.36 (s, 2 H, Ar) ppm. ^{13}C NMR (400 MHz, CD_3OD): δ = 13.43 (CH_3 chain), 22.73, 22.94, 26.58, 29.36, 29.47, 29.61, 29.66, 29.74, 32.06 (CH_2 chain), 49.84 [$N^+(CH_3)_2$], 56.07 (ArOCH_3), 62.02 (ArCH_2N^+), 65.61 (RCH_2N^+), 118.49 (Ar), 120.00 (*ipso*-*Ar*CH_2N^+), 153.34 (OAr-*ipso*) ppm. Br calcd. 21.28%; found 21.22%.

Preparation of the SWNTs Dispersions: Aqueous dispersions of SWNTs were prepared by adding aqueous dispersant solutions (5 mL) of different concentrations to pristine SWNTs (1 mg) in a glass centrifuge tube. The sample was then sonicated with an ultrasonic bath (Transsonic 310 Elma, 35 KHz) for several hours. The

obtained suspension was centrifuged for 15 min at 4000 RPM using a Universal 32 (Hettich Zentrifugen) centrifuge in order to favour the separation of the supernatant aqueous solution from the precipitate. We ascertained that sonication did not damage the surfactant by comparing the UV/Vis spectra of the solutions recorded at different sonication times. Figures S8–S10 show no evidence of molecular damage during sonication. The optimum sonication time was chosen by preparing a dispersion of SWNTs (1 mg) with the appropriate amount of surfactant and sonicating (at 35 kHz) for a variable time (1 to about 6 h). As highlighted from the example in Figure S11, the absorbance of dispersed SWNTs increases upon increasing the sonication time (up to 4–5 h, depending on the investigated surfactant) and then remains essentially unchanged (up to 6 h). Consequently, a sonication time of 5 h can be considered a fair compromise at all the concentrations of surfactants. It must be pointed out that the sonication process usually leads to a moderate increase in the temperature of the sample, which might further favour the dispersion of SWNTs.

NIR-PL Measurements: NIR-PL studies were carried out on supernatants ($[SWNTs]_i$ = 0.2 mg/mL, [dispersant] = 1 mM, sonication time 5 h) diluted 1:10 with a L.O.T. ORIEL NS1 NanoSpectralyzer® (diode lasers; λ_{exc} = 638, 683 and 785 nm) with an integration time of 1 s and five accumulations. NIR-PL efficiency data represent the spectrally integrated emission values adjusted to the fraction of excitation light absorbed by the sample. The emission efficiency (*ee*) was determined for the three λ_{exc} according to Equation (1), where the total emission power value corresponds to the integer of the total NIR emission spectrum.

$$ee = \text{total emission power/absorption at } \lambda_{exc} \quad (1)$$

Raman Determinations: Micro-Raman scattering measurements were carried out at room temperature in the backscattering geometry using a Renishaw 1000 micro-Raman system equipped with a CCD camera and Leica microscope. An 1800 lines mm^{-1} grating was used for all measurements, providing a spectral resolution of ca. 1 cm^{-1}. A He-Ne laser excitation source with 488 and 633 nm excitations with variable power was used. Measurements were taken with 20 seconds of exposure time and two accumulations. The laser spot was focused on the sample surface using a 50× objective with short-focus working distance. Raman spectra were collected from numerous spots of the sample and recorded with a Peltier cooled CCD camera. Only one spectrum was collected per spot. The data were collected and analyzed with Renishaw Wire and GRAMS software.

UV/Vis/NIR Spectroscopic Characterization of SWNT Dispersion: The absorption spectra of the suspended SWNTs were recorded with a Varian Cary 100 Bio UV/Vis spectrophotometer using 1 mm path length quartz cuvettes. To quantify the amount of dispersed SWNTs, we used the previously determined[23] extinction coefficient of 106.0 ± 1.3 $mL\,mg^{-1}\,cm^{-1}$ at 377 nm. The behaviour of the suspensions in the NIR region was examined with a Jasco V-570 UV/Vis/NIR spectrophotometer.

ζ-Potential Measurements: The ζ-potentials of the SWNT solutions were measured using a Zeta Plus apparatus (Zeta Potential Analyzer, Brookhaven Instruments Corporation). Solutions of ca. 0.1 mg/mL SWNTs and 1 mM surfactant were diluted, applying ultasonication, 1:5 in order to perform the measurements. The ionic strength was kept constant at 10 mM (NaCl).

Supporting Information (see footnote on the first page of this article): NIR–PL spectra of SWNTs solubilized with the investigated surfactants upon excitation at 683 and 785 nm; full range Raman spectra of raw SWNTs and SWNTs dispersed with surfactants upon excitation 633 nm; RBM bands in the Raman spectra upon excitation at 633 nm before and after washing with acetone; stability of the aqueous dispersions of SWNTs over time; UV/Vis spectra of the investigated surfactants subjected to different sonication times; UV/Vis spectra of SWNTs dispersed with 1 mM pDOT-ABr recorded at different sonication times.

Acknowledgments

We thank Prof. Maurizio Prato for supplying raw nanotubes and for useful discussion and Dr. Diana Velluto for ζ-potential measurements. This work has been supported by Ministero dell'Università e della Ricerca (MIUR) (PRIN 2008, prot. 20085M27SS). The authors wish to acknowledge financial support by the Science Foundation Ireland (SFI) (PIYRA 07/YI2/I1052), Irish Research Council for Science, Engineering and Technology (IRCSET), and Intel (Postgraduate Research Scholarships to E. D. C.).

[1] a) N. R. Wilson, J. V. MacPherson, *Nat. Nanotechnol.* **2009**, *4*, 483–491; b) B. S. Shim, J. Zhu, E. Jan, K. Critchley, S. Ho, P. Podsiadlo, K. Sun, N. A. Kotov, *ACS Nano* **2009**, *3*, 1711–1722.
[2] Y. Yun, Z. Dong, V. Shanov, W. R. Heineman, H. B. Halsall, A. Bhattacharya, L. Conforti, R. K. Narayan, W. S. Ball, M. J. Schulz, *Nano Today* **2007**, *2*, 30–37.
[3] Z. Liu, K. Chen, C. Davis, S. Sherlock, Q. Cao, X. Chen, H. Dai, *Cancer Res.* **2008**, *68*, 6652–6660.
[4] J. Li, L. Q. Zhang, *Mater. Sci. Technol.* **2011**, *27*, 252–256.
[5] a) B. J. Landi, R. P. Raffaelle, M. J. Heben, J. L. Alleman, W. VanDerveer, T. Gennett, *Nano Lett.* **2002**, *2*, 1329–1332; b) T. Fukushima, K. Asaka, A. Kosaka, T. Aida, *Angew. Chem. Int. Ed.* **2005**, *44*, 2410–2413.
[6] I. Guryanov, F. M. Toma, A. Montellano López, M. Carraro, T. Da Ros, G. Angelini, E. D'Aurizio, A. Fontana, M. Maggini, M. Prato, M. Bonchio, *Chem. Eur. J.* **2009**, *15*, 12837–12845.
[7] M. Prato, K. Kostarelos, A. Bianco, *Acc. Chem. Res.* **2008**, *41*, 60–68.
[8] Z. Liu, S. Tabakman, K. Welsher, H. Dai, *Nano Res.* **2009**, *2*, 85–120.
[9] a) C. Tripisciano, K. Kraemer, A. Taylor, E. Borowiak-Palen, *Chem. Phys. Lett.* **2009**, *478*, 200–205; b) J. Chen, S. Chen, X. Zhao, L. V. Kuznetsova, S. S. Wong, I. Ojima, *J. Am. Chem. Soc.* **2008**, *130*, 16778–16785; c) Y. Krupskaya, C. Mahn, A. Parameswaran, A. Taylor, K. Krämer, S. Hampel, A. Leonhardt, M. Ritschel, B. Büchner, R. Klingeler, *J. Magn. Magn. Mater.* **2009**, *321*, 4067–4071.
[10] M. J. Rosen, *Surfactants and Interfacial Phenomena*, Wiley, New York, 2nd ed., **1989**.
[11] F. M. Menger, J. S. Keiper, *Angew. Chem. Int. Ed.* **2000**, *39*, 1906–1920.
[12] a) P. H. Elworty, A. I. Florence, C. B. Macfalane, *Solubilization by Surface-Active Agents and Its Application in Chemistry and the Biological Sciences*, Chapman & Hall, London, **1968**; b) C. A. Miller, *Handbook of Surface and Colloid Chemistry*, CRC, **2008**, pp. 415–438 (chapter: Solubilization in Surfactant Systems).
[13] M. F. Islam, E. Rojas, D. M. Bergey, A. T. Johnson, A. G. Yodh, *Nano Lett.* **2002**, *3*, 269–273.
[14] O. Matarredona, H. Rhoads, Z. R. Li, J. H. Harwell, L. Balzano, D. E. Resasco, *J. Phys. Chem. B* **2003**, *107*, 13357–13367.
[15] K. Yurekli, C. A. Mitchell, R. Krishnamoorti, *J. Am. Chem. Soc.* **2004**, *126*, 9902–9903.
[16] a) M. J. O'Connell, S. M. Bachilo, C. B. Huffman, V. C. Moore, M. S. Strano, E. H. Haroz, K. L. Rialon, P. J. Boul, W. H. Noon, C. Kittrell, J. Ma, R. H. Hauge, R. B. Weisman, R. E.

Smalley, *Science* **2002**, *297*, 593–596; b) Y. Kang, T. A. Taton, *J. Am. Chem. Soc.* **2003**, *125*, 5650–5651; c) A. Di Crescenzo, M. Aschi, E. Del Canto, S. Giordani, D. Demurtas, A. Fontana, *Phys. Chem. Chem. Phys.* **2011**, *13*, 11373–11383.
[17] Y. Han, Y. Wang, *Phys. Chem. Chem. Phys.* **2001**, *13*, 1939–1956.
[18] Q. Wang, Y. Han, Y. Qin, Z.-X. Guo, *J. Phys. Chem. B* **2008**, *112*, 7227–7233.
[19] L. Chen, H. Xie, Y. Li, W. Yu, *Colloid Surf., A: Physicochem. Eng. Asp.* **2008**, *330*, 176–179.
[20] a) G. J. Bahun, C. Wang, A. Adronov, *J. Polym. Sci. Pol. Chem.* **2006**, *44*, 1941–1951; b) D. M. Guldi, G. M. A. Rahman, N. Jux, D. Balbinot, U. Hartnagel, N. Tagmatarchis, M. Prato, *J. Am. Chem. Soc.* **2005**, *127*, 9830–9838.
[21] N. Nakashima, Y. Tomonari, H. Murakami, *Chem. Lett.* **2002**, *31*, 638–639.
[22] C. Ehli, G. M. A. Rahman, N. Jux, D. Balbinot, D. M. Guldi, F. Paolucci, M. Marcaccio, D. Paolucci, M. Melle-Franco, F. Zerbetto, S. Campidelli, M. Prato, *J. Am. Chem. Soc.* **2006**, *128*, 11222–11231.
[23] A. Di Crescenzo, D. Demurtas, A. Renzetti, G. Siani, P. De Maria, M. Meneghetti, M. Prato, A. Fontana, *Soft Matter* **2009**, *5*, 62–66.
[24] S. Attal, R. Thiruvengadathan, O. Regev, *Anal. Chem.* **2006**, *78*, 8098–8104.
[25] L. Brinchi, R. Germani, L. Goracci, G. Savelli, C. A. Bunton, *Langmuir* **2002**, *18*, 7821–7825.
[26] L. Brinchi, R. Germani, G. Savelli, L. Marte, *J. Colloid Interf. Sci.* **2003**, *262*, 290–293.
[27] J. E. Brady, D. F. Evans, G. G. Warr, F. Grieser, B. W. Ninham, *J. Phys. Chem.* **1986**, *90*, 1853–1859.
[28] L. Jiang, L. Gao, J. Sun, *J. Colloid Interf. Sci.* **2003**, *260*, 89–94.
[29] R. B. Weisman, S. M. Bachilo, *Nano Lett.* **2003**, *3*, 1235.
[30] a) C. Fantini, A. Jorio, M. Souza, M. S. Strano, M. S. Dresselhaus, M. Pimenta, *Phys. Rev. Lett.* **2004**, *93*, 147406/1–147406/4; b) J. Maultzsch, H. Telg, S. Reich, C. Thomsen, *Phys. Rev. B* **2005**, *72*, 205438/1–205438/16.
[31] P. C. Hiemez, R. Rajagopalan, *Principles of Colloid and Surface Chemistry*, Marcel Dekker, New York, 3rd ed., **1997**.

Received: May 23, 2011
Published Online: ■

EurJOC European Journal of Organic Chemistry

Gemini surfactants with a rigid spacer are demonstrated to be good dispersing agents for single-walled carbon nanotubes at very low surfactant concentrations.

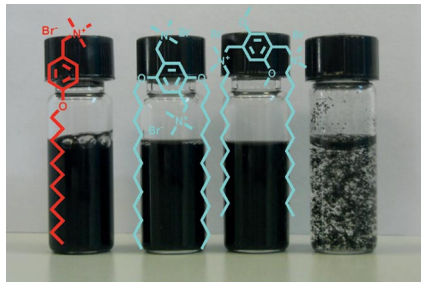

Keywords: Nanotechnology / Nanotubes / Semiconductors / Surfactants / Raman spectroscopy

